Journal of Materials Science: Materials in Electronics (2018) 29:12978–12985
https://doi.org/10.1007/s10854-018-9418-0

Temperature stable microwave dielectric ceramics in $Li_2ZnTi_3O_8$–based composite for LTCC applications

Haishen Ren[1,2] · Haiyi Peng[1,3] · Tianyi Xie[1] · Liang Hao[1] · Mingzhao Dang[1,3] · Xie Meng[2] · Shaohu Jiang[1] · Yi Zhang[1] · Huixing Lin[1] · Lan Luo[1]

Received: 23 April 2018 / Accepted: 1 June 2018 / Published online: 4 June 2018

Abstract
A temperature stable low temperature co-fired ceramic (LTCC) was fabricated by the powder mixture of $Li_2ZnTi_3O_8$ ceramic, TiO_2 τ_f-tailoring dopant and B_2O_3–La_2O_3–MgO–TiO_2 (BLMT) glass sintering aid, and the sintering behavior, activation energy, phase composition, microstructure and microwave dielectric properties of the composite were investigated in the composition range (wt%) of 5 BLMT–(95-x) $Li_2ZnTi_3O_{8-X}$ TiO_2 (x = 0, 1, 2, 3, 4 and 5). The sintering behavior results showed that all composites could be well sintered at 910 °C for 2 h through liquid-phase sintering. The activation energy of $Li_2ZnTi_3O_8$ ceramic was calculated to be 520.9 ± 40.46 kJ/mol, while 5BLMT–93$Li_2ZnTi_3O_8$–2TiO_2 (in wt%) composite was reduced to 330.98 ± 47.34 kJ/mol. The XRD results showed that $Li_2ZnTi_3O_8$ and TiO_2 phase stably existed in all sample and a new phase $LaBO_3$ was crystallized from BLMT glass during sintering process. As x increases, the rutile TiO_2 phase increased in composite, which could adjust the temperature coefficient of resonant frequency (τ_f) to near-zero owing to the opposite τ_f value to other phases. And simultaneously dielectric constant (ε_r) demonstrated gradually increase, whereas the quality factor (Q × f) decreased gradually. The composite with x = 2 had an optimal microwave dielectric properties with ε_r = 25.3, Q × f = 32,800 GHz, and τ_f = − 0.54 ppm/°C. The corresponding fitting equations of ε_r, Q × f and τ_f on the x value were obtained by the Origin software, indicating that the dielectric properties of the composite could be precisely controlled by varying the content of TiO_2. In addition, the good chemical compatibility of this material with Ag electrode made it as a potential candidate for LTCC technology.

1 Introduction

For meeting the requirements of high-miniaturization, high-reliability, and multifunctional performance of microwave devices, low-temperature co-fired ceramics (LTCC) technology has been playing an increasingly significant role in the development to Internet of Things, the Tactile Internet (5th generation wireless systems), electronic warfare, satellite broadcasting and intelligent transport systems [1, 2]. The ideal LTCC materials owe several features such as low sintering temperature (below 950 °C), an appropriate dielectric constant (ε_r), high quality factor (Q × f) and a near-zero temperature coefficient of resonant frequency ($|\tau_f| \leq 10$ ppm/°C) [3]. Unfortunately, most of the dielectric ceramics with good microwave dielectric properties cannot be used for LTCC application due to the sintering temperatures above 1000 °C. Therefore, one of the most important focal problems for the development of LTCC materials is to lower the sintering temperature and maintain the excellent dielectric properties of the ceramics as much as possible.

Recently, the dielectric ceramics in the Li_2O–ZnO–TiO_2 ternary system have drawn more attention due to its good microwave dielectric properties and the excellent chemical compatibility with Ag inner electrodes. And among them, $Li_2ZnTi_3O_8$ (L_2ZT_3) ceramic has excellent microwave dielectric properties with middle-dielectric constant (25.6), excellent quality factor (72,000 GHz) and negative temperature coefficient of resonant frequency (− 11.2 ppm/°C)

✉ Haishen Ren
renhaichen@student.sic.ac.cn

✉ Huixing Lin
huixinglin@mail.sic.ac.cn

[1] Key Laboratory of Inorganic Functional Material and Device, Shanghai Institute of Ceramics, Chinese Academy of Sciences, Shanghai 200050, China

[2] CAS Key Laboratory of Materials for Energy Conversion, Chinese Academy of Sciences, Shanghai 200050, China

[3] University of Chinese Academy of Sciences, Beijing 100049, China

[4, 5]. Obviously, the sintering temperature (1075 °C) and τ_f value are a huge barrier for it to be further applied in LTCC technology. In order to realize $Li_2ZnTi_3O_8$ ceramics for LTCC applications, low-melting sintering aids such as Bi_2O_3 and $ZnO–La_2O_3–B_2O_3$ glass for lowering the sintering temperature and a positive τ_f-tailoring material (e.g. TiO_2 + 465 ppm/°C, $CaTiO_3$ + 174 ppm/°C) for modifying to near-zero τ_f value are used simultaneously [6–9]. It can be found from our previous works that $B_2O_3–La_2O_3–MgO–TiO_2$ (BLMT) glass is a promising sintering aid for lowering the sintering temperature of ceramics (for instance, $BaTiO_4$ and $Li_2Zn_3Ti_4O_{12}$) due to its low transformation temperature (644 °C) [10, 11]. In addition, TiO_2 is chosen as the positive τ_f-tailoring material in this study. In this paper, a series of LTCC composites based on 5 BLMT–(95-x) $Li_2ZnTi_3O_{8-X}$ TiO_2 (x = 0, 1, 2, 3, 4 and 5, in wt%) are fabricated, meanwhile the effects of the TiO_2 on the crystallization, microstructure and microwave dielectric properties of the material are investigated.

2 Experimental

$Li_2ZnTi_3O_8$ phase was prepared by the solid-state-reaction method. Stoichiometry of Li_2CO_3, ZnO and TiO_2 (99.9%) were weighted and mixed in a Nylon tank using ethyl alcohol and ZrO_2 balls as media by planetary ball mill for 2 h. The mixture was then dried and calcined at 900 °C for 4 h to form $Li_2ZnTi_3O_8$ phase. The BLMT glass with the molar composition of $3B_2O_3–1.2La_2O_3–1.8MgO–1TiO_2$ was prepared by a conventional glass fabrication process. The glass batch about 300 g was melted in a platinum crucible at 1350 °C for 1.5 h, and then the melts were quenched in water. The quenched glass was planetary-milled in aluminum jar with ethyl alcohol and ZrO_2 balls for 2 h. After being dried and screened through a 200-mesh sieve, the BLMT glass powder was obtained. Last, the BLMT glass powder, calcined $Li_2ZnTi_3O_8$ powder and TiO_2 powder were weighed with the ratio of 5 BLMT–(95−x) $Li_2ZnTi_3O_{8-X}$ TiO_2 (x = 0, 1, 2, 3, 4 and 5, in wt%) and planetary-milled with ZrO_2 balls and ethyl alcohol for 1 h. After drying, the mixture was granulated by adding 8 wt% poly(vinyl butyral) (PVB) solution for getting the uniformity particle size and good fluidity power. Preformed pellets of 15 mm in diameter and 8 mm in height were obtained from the powder using a cylindrical steel mold, and then were pressed at 2 MPa by hydraulic pressing, followed by sintering between 550 and 920 °C for 2 h in air at a heating rate of 5 °C/min.

Shrinkage process was measured with 18/5.0/5.0 cm^3 "green" samples by using a horizontal-loading dilatometer with alumina rams and boats (DIL 402C, Netzsch Instruments, Germany) with different heating rate of 5, 10 and 15 K/min, respectively. The bulk density of sintered samples was measured applying the Archimedes method. The crystalline phase present in sintered samples was identified by X-ray diffraction analysis (XRD, D8 ADVANCE, Bruker, Germany) using a Cu/Kα radiation, and was further analyzed by energy dispersive spectroscopy (EDS, Magellan 400, FEI Company, USA). The microstructure characteristics of the sintered samples was observed by field emission scanning electron microscope (FESEM, Magellan 400, FEI Company, USA). The dielectric constant and tan δ (dielectric loss) of the samples with the diameter of 12 mm and the height of 6 mm were collected by the Hakki–Coleman dielectric resonator method in the TE011 mode using an Agilent E8363A PNA series network analyzer. The Q value were calculated from the value in the light of the Q = 1/tan δ. The τ_f value was measured over the range from 25 to 85 °C heating through the temperature test cabinet (VTL7003, Vötsch, Germany), and was calculated by following equation:

$$\tau_f = \left(f_{85} - f_{25}\right) / \left(60 \times f_{25}\right) \times 10^6 (ppm/°C) \quad (1)$$

where f_{85} and f_{25} represent the resonant frequencies at 85 and 25 °C, respectively.

3 Results and discussion

Figure 1a shows the linear shrinkage curves of the L_2ZT_3 ceramic and the L_2ZT_3–BLMT–TiO_2 (x = 2) composite at different heating rates of 5, 10 and 15 K/min. The shrinkage of pure L_2ZT_3 ceramic starts at 950 °C and a linear shrinkage of 16% at 1150 °C, while the onset of shrinkage dramatically decreases to about 640 °C for BLMT doped composites, which is in agreement with our previous reports that the shrinkage of composites containing the BLMT glass approximately starts at the temperature of glass transformation [10, 11], and ends in 18% of shrinkage at 960 °C. It can be easily seen that the BLMT glass can efficiently reduce the sintering temperature of the ceramic due to the presence of the liquid phase. These observations are further supported by the bulk density of composites with different TiO_2 content as a function of sintering temperature range from 650 to 920 °C for 2 h, as shown in Fig. 1b. The bulk density of composite with < 2.0 g/cm^3 keep a slow increasing tendency as sintering temperature increasing from 650 to 700 °C. When the sintered temperature rises from 700 to 910 °C, the bulk density of the composite rapid increases to about 3.75 g/cm^3 and reaches a maximum value sintered at 910 °C, then slightly decreases due to over-heating. All the results from Fig. 1 demonstrate that the densification of BLMT–$Li_2ZnTi_3O_8$–TiO_2 composites can be obtained by sintering at 910 °C for 2 h.

To further understand the sintering behavior, the activation energy (Ea) of the L_2ZT_3–BLMT–TiO_2 (x = 2)

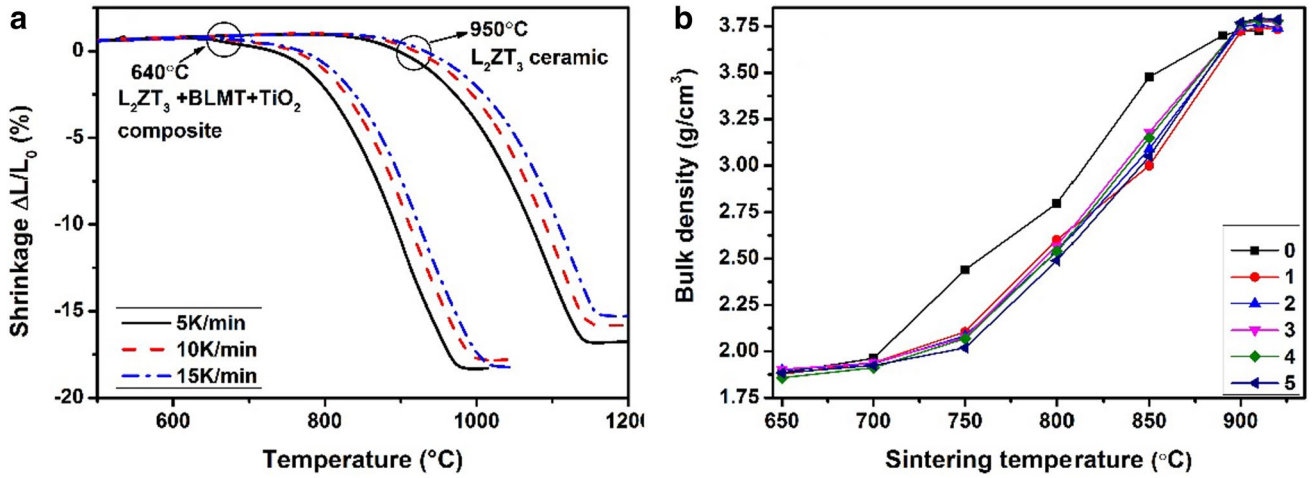

Fig. 1 **a** Liner shrinkage curves of the L_2ZT_3 ceramic and the L_2ZT_3-BLMT–TiO_2 (x = 2) composite at different heating rates of 5, 10 and 15 K/min. **b** The bulk density of composites with different TiO_2 content sintered at different temperatures for 2 h

composite and the L_2ZT_3 ceramic can be calculated by the follow Arrhenius equation [12, 13]:

$$lnk = -E_a/R(1/T) + lnz \quad (2)$$

in which Ea is the activation energy, k is the heating rate, T is the absolute temperature, R is the universal gas constant (8.3145 J/K/mol) and lnz is a constant. The Ea values can be obtained by plotting lnk vs 1/T. Figure 2 shows the lnk plotted against 1/T for the L_2ZT_3–BLMT–TiO_2 (x = 2) composite (a) and the L_2ZT_3 ceramic (b) at a given shrinkage values (dL/L_0), 3, 6, 9, 12 and 15% according to Fig. 1a. After calculated from the dilatometric curves, an average Ea of about 389.14 ± 51.73 kJ/mol for the L_2ZT_3–BLMT–TiO_2 (x = 2) composite and an average Ea of about 450.05 ± 58.88 kJ/mol for the L_2ZT_3 ceramic are obtained (Table 1), which indicates that the activation energy is significantly reduced when L_2ZT_3 ceramic sintering at low temperature doping with BLMT glass. It is similar with the report [13, 14] that the liquid-phase sintering mechanism enhanced the sintering process should lead to a decrease of the Ea.

Figure 3 shows XRD patterns of the composites with different TiO_2 content sintered at 910 °C for 2 h. It can be found from the Fig. 3 that the peaks belonging to orthorhombic $LaBO_3$ (JCPDS File No. 12-0762) phase are indexed in all as-sintered sample besides a cubic structure $Li_2ZnTi_3O_8$ (JCPDS No. 44-1037) phase. According to our previous work [10, 11], BLMT glass can crystallize forming the $LaBO_3$ phase at sintering temperature above 700 °C. As x value increases from 1 to 5, the peaks of rutile TiO_2 (JCPDS File No. 21-1276) phase appears besides $Li_2ZnTi_3O_8$ and $LaBO_3$ and the peak intensity become more obvious with x increasing. It means the positive τ_f-tailoring material TiO_2 does not chemically react with the BLMT glass or $Li_2ZnTi_3O_8$ ceramic, which is a

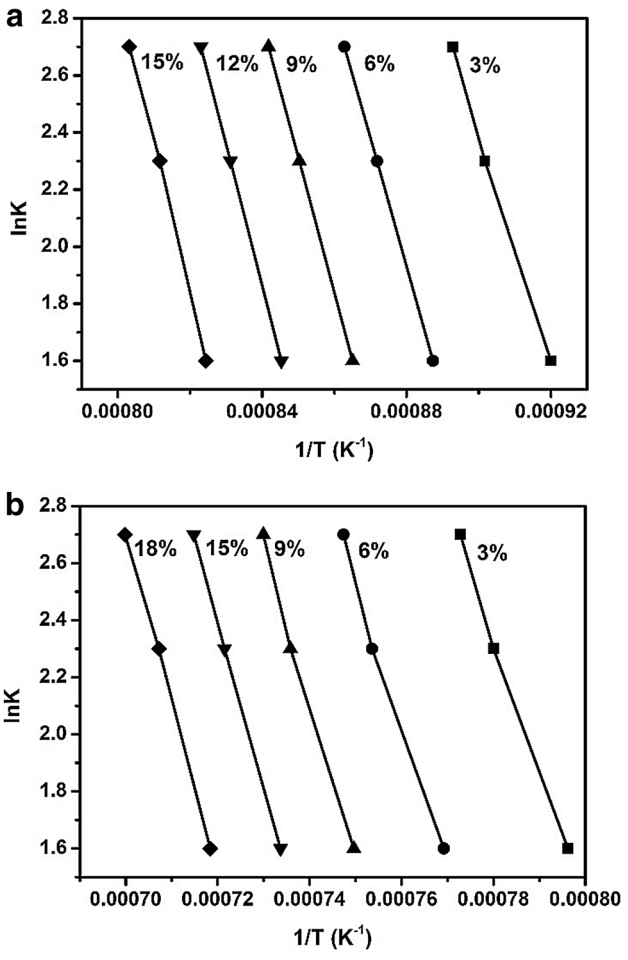

Fig. 2 The lnk plotted against the inverse of temperature (1/T) for the L_2ZT_3–BLMT–TiO_2 (x = 2) composite (**a**) and the L_2ZT_3 ceramic (**b**) at a given shrinkage values

Table 1 The activation energy of the L_2ZT_3–BLMT–TiO_2 (x = 2) composite and the L_2ZT_3 ceramic at a given shrinkage values

Shrinkage dL/L_0(%)	Activation energy of the L_2ZT_3–BLMT–TiO_2 (x = 2) composite (kJ/mol)	Activation energy of the L_2ZT_3 ceramic (kJ/mol)
3	337.41	391.17
6	373.32	418.64
9	392.51	464.3
12	410.81	484.44
15	431.63	491.7
Average	389.14 ± 51.73	450.05 ± 58.88

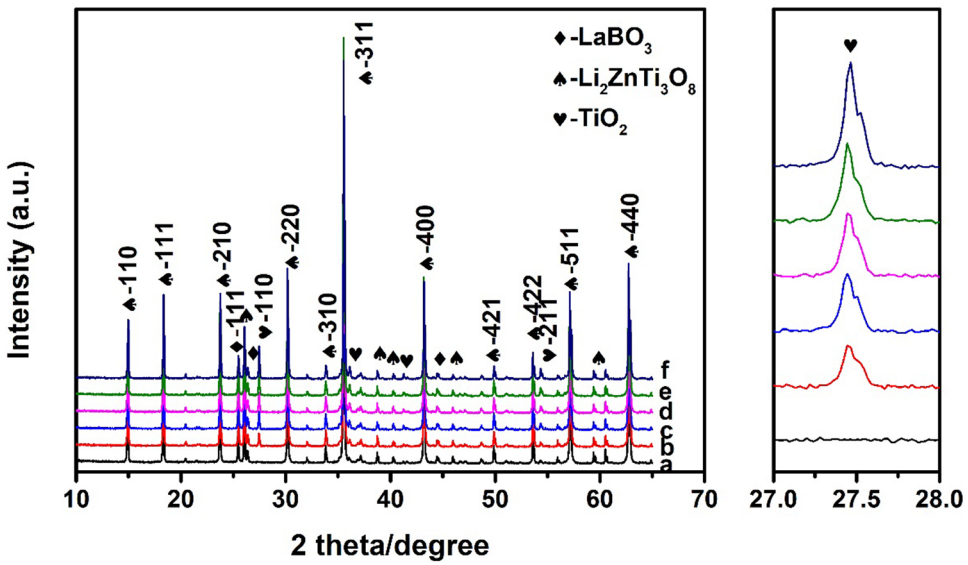

Fig. 3 XRD patterns of the composites with different TiO_2 content: 0 (**a**), 1 (**b**), 2 (**c**), 3 (**d**), 4 (**e**) and 5 wt% (**f**) sintered at 910 °C for 2 h

great advantage to modify the τ_f value of the composite to near-zero.

Figure 4 illustrates the backscattered electron micrograph of the composites with different TiO_2 contents sintered at 910 °C for 2 h. The well-densified microstructures are obtained and little porosity is observed in all sintered samples. It can be found from Fig. 3a that the composite are composed of two kinds of grains with different contents without TiO_2 exhibits compact microstructure with grain sizes in the range 10–40 μm. The result of EDS analysis in Fig. 5 shows that big and gray grains (marked A) are dominantly composed of O, Ti, and Zn elements, and the Li element belongs to the ultra-light elements so that it cannot be detected by EDS [15]. The ratio of Zn:Ti is about 1:3, which is consistent with the composition of $Li_2ZnTi_3O_8$. And small and white grains (marked B) mainly contain B, La, and O elements in an approximate molar ratio of B:La = 1:1, suggesting that grains belong to the $LaBO_3$ phase, which agree well with the analysis of X-ray diffraction patterns. However, some fine grains are observed in all samples containing TiO_2 compared with the specimen without TiO_2, as shown in Fig. 5 b–f. The fine grains becomes more with increasing TiO_2 contents, which may be contributed by its high sintering temperature (above 1300 °C). In particular, a small amount of tetragonal rutile TiO_2 are firstly observed in Fig. 3 f according to the EDS analysis in Fig. 5 (at x = 5). The contrast of $Li_2ZnTi_3O_8$ and TiO_2 is close because of the average atomic number of $Li_2ZnTi_3O_8$ (11.06) and TiO_2 (12.67), which lead to the difficulty to distinguish between $Li_2ZnTi_3O_8$ and TiO_2 phase.

The variations of the dielectric constant (a), Q × f (b) and τ_f valve (c) of composites sintered at 910 °C/2 h with different TiO_2 content are shown in Fig. 6, respectively. It can be easily seen from Fig. 6a that dielectric constant increases from 24.5 to 26.5 with increases of TiO_2 content from 0 to 5 wt%. In generally, the ε_r values of composite ceramics is mainly affected by its phase composition according to the equation of mixture rules:

$$\ln \varepsilon_r = x_1 \ln \varepsilon_{r1} + x_2 \ln \varepsilon_{r2} + \ldots + x_i \ln \varepsilon_{ri} \quad (3)$$

where ε_{ri} and x_i are the ε_r and volume fraction of the i phase, respectively. On the basis of the previous phases study as shown in Fig. 3 and Table 2, the increase in ε_r with the contents of x can be explained by the increase of the higher-ε_r TiO_2 (104) and the decrease of $Li_2ZnTi_3O_8$ in composites. As the single-phase $Li_2ZnTi_3O_8$ has a much bigger

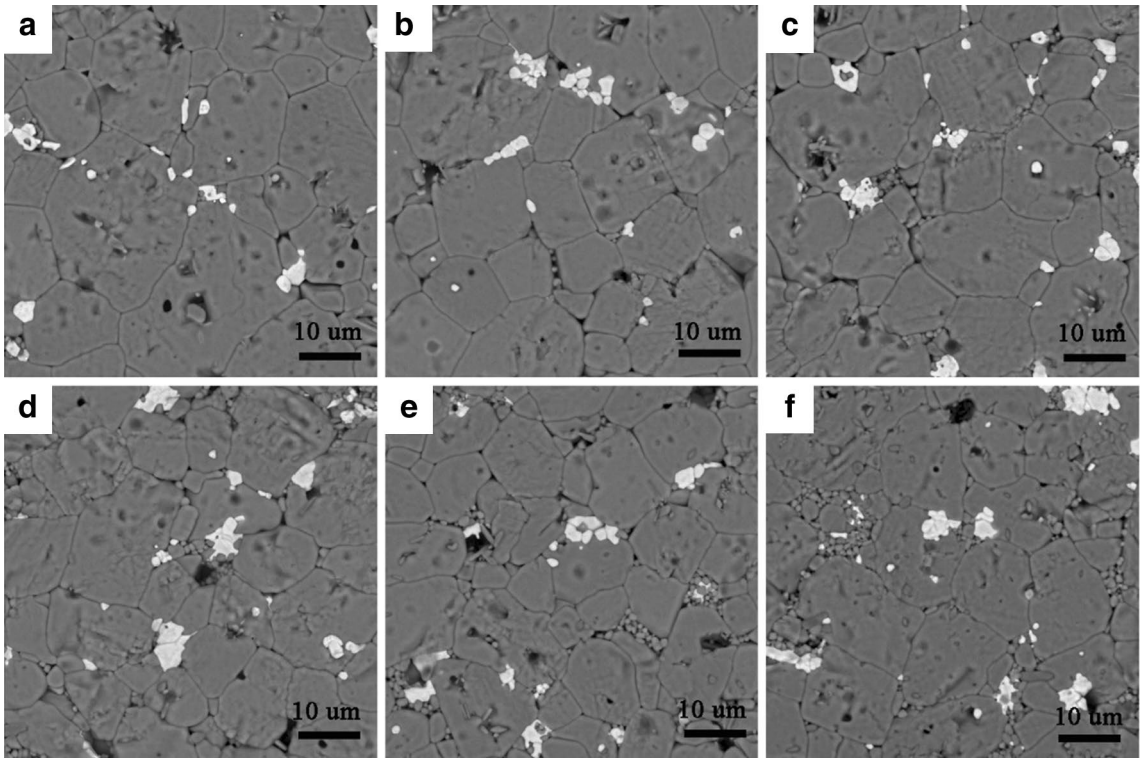

Fig. 4 Backscattered electron micrograph of the composites with 0 (**a**), 1 (**b**), 2 (**c**), 3 (**d**), 4 (**e**) and 5 wt% (**f**) sintered at 910 °C for 2 h

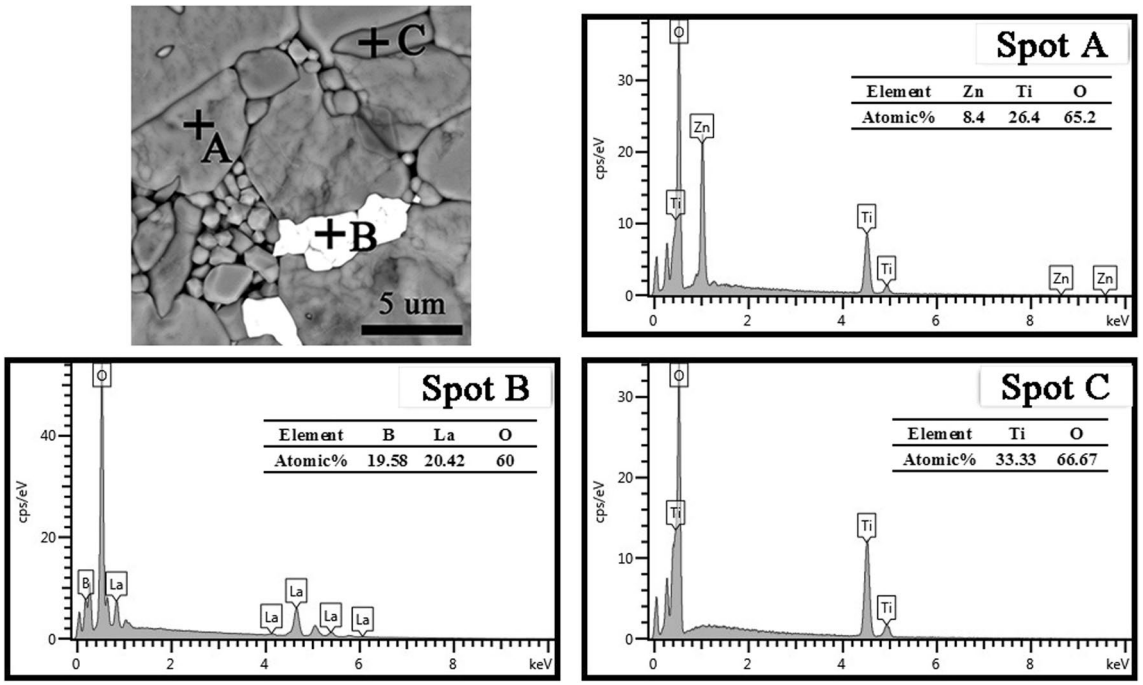

Fig. 5 EDX analysis and data on the marked areas of the composites with 5 wt% TiO_2 for 910°C/2 h

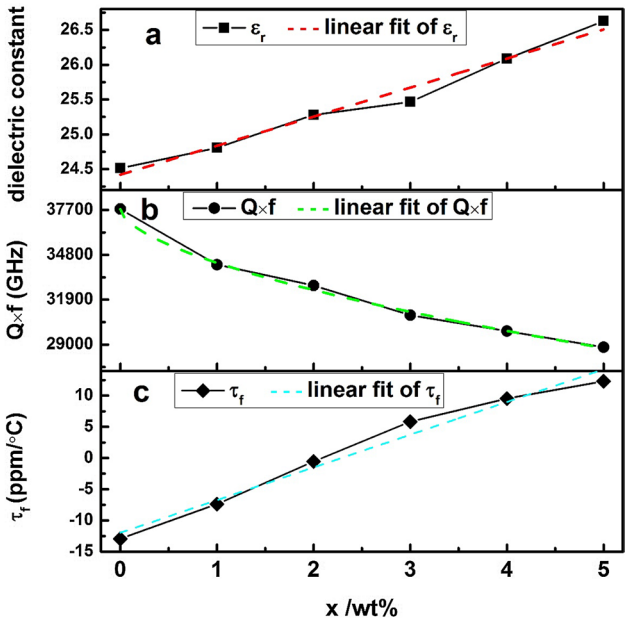

Fig. 6 The dielectric constant (**a**), Q×f (**b**) and τ_f values (**c**) of the composites with different TiO_2 content sintered at 910 °C for 2 h

Q×f value than TiO_2 phase as shown in Table 2, the Q×f value of the composites generally decrease from 37,700 to 29,000 GHz with increasing the content of TiO_2 as shown in Fig. 6b. The variation of the τ_f values with TiO_2 content has a similar tendency with dielectric constants shown in Fig. 6c. The τ_f of composites is well known to be influenced by the composition and their relative contents [15–17]. It is easily found that the τ_f valve increases − 12.94 to + 12.31 ppm/°C due to the increasing of TiO_2 phase (+456 ppm/°C). On the whole, the promising microwave dielectric properties of $\varepsilon_r = 25.3$, Q×f = 32,800 GHz, and $\tau_f = -0.54$ ppm/°C can be obtained when the composites with x = 2 is sintered at 910 °C for 2 h. Compared with other $Li_2ZnTi_3O_8$ LTCC materials as listed in Table 3, 5 BLMT-93 $Li_2ZnTi_3O_8$–2 TiO_2 (in wt%) composite can be sintered at a lower temperature and possesses a near-zero temperature coefficient of resonant frequency.

In particular, it is worth to pointing out that the dielectric properties of composites seem to be a linear relationship with the TiO_2 content. Based on the experimental data in Fig. 6, the corresponding fitting equations of ε_r, Q×f and τ_f on the TiO_2 content are obtained by the Origin software:

$$y_{\varepsilon r} = 24.42067 + 0.4174x \quad \left(Adj.R^2 = 0.9733\right) \tag{4}$$

$$y_{Q\times f} = -508420 + 546180 \Big/ \left[1 + \left({}^{x}/_{4820}\right)^{0.59557}\right]$$

$$\left(Adj.R^2 = 0.99305\right) \tag{5}$$

$$y_{\tau f} = -11.9619 + 5.2394x \quad (Adj.R - Square = 0.97306) \tag{6}$$

It can be found from these equations that ε_r and τ_f value are linear with the TiO_2 content and there is a logistic regression equation of Q×f value on the TiO_2 content, which indicates that the dielectric properties can be precisely adjusted by adding the suitable content of TiO_2. For instance, when $y_{\tau f} = 0$, τ_f of composite is zero, the x value is 2.28 and $\varepsilon_r = 25.37$, Q×f = 32,766 GHz according to Eqs. (4), (5) and (6). This results also confirm that the ε_r and τ_f value of composites are mainly influenced by the phase composition and their relative contents in composites, therefor there are a linear relationship between the ε_r and τ_f value and relative

Table 2 Microwave dielectric properties, density and sintering temperature of compounds in composites

	ε_r	Q × f (GHz)	τ_f (ppm/°C)	Density (g/cm^3)	Ts (°C)	References
$LaBO_3$	12.5	56,000	− 52	4.25	1200	[18]
$Li_2ZnTi_3O_8$	25.6	72,000	− 11.2	3.974	1075	[4]
TiO_2	104	44,000	+456	5.304	1300	[9]

Ts Sintering temperature

Table 3 Comparison of sintering temperature and dielectric properties of recently reported $Li_2ZnTi_3O_8$ LTCC materials with this study

Composition	ε_r	Q × f (GHz)	τ_f (ppm/°C)	Ts (°C)	References
1 wt% CBS glass + 4 wt% TiO_2 + $Li_2ZnTi_3O_8$	26.9	23,563	− 1.5	900/4 h	[19]
1 wt% LZB glass + 3.5 wt% TiO_2 + $Li_2ZnTi_3O_8$	26.1	45,168	− 4.1	900/4 h	[20]
4 wt% Li_2WO_4 + 4 wt% TiO_2 + $Li_2ZnTi_3O_8$	27.1	51,123	− 3.8	860/4 h	[8]
1.5 wt% B_2O_3 + 3 wt% TiO_2 + $Li_2ZnTi_3O_8$	25.9	46,487	− 0.35	900/4 h	[21]
1 wt% LAB glass + 17 mol% TiO_2 + $Li_2ZnTi_3O_8$	26.8	28,000	+2.5	900/4 h	[22]
1 wt% LBS glass + 3.5 wt% TiO_2 + $Li_2ZnTi_3O_8$	26	44,023	− 4.4	950/4 h	[23]
1 wt% ZBS glass + 0.6$Li_2ZnTi_3O_8$–0.4Li_2TiO_3	25.4	86,400	− 1.0	900/4 h	[24]
5 BLMT–93 $Li_2ZnTi_3O_8$–2 TiO_2 (in wt%)	25.3	32,800	− 0.54	910/2 h	This paper

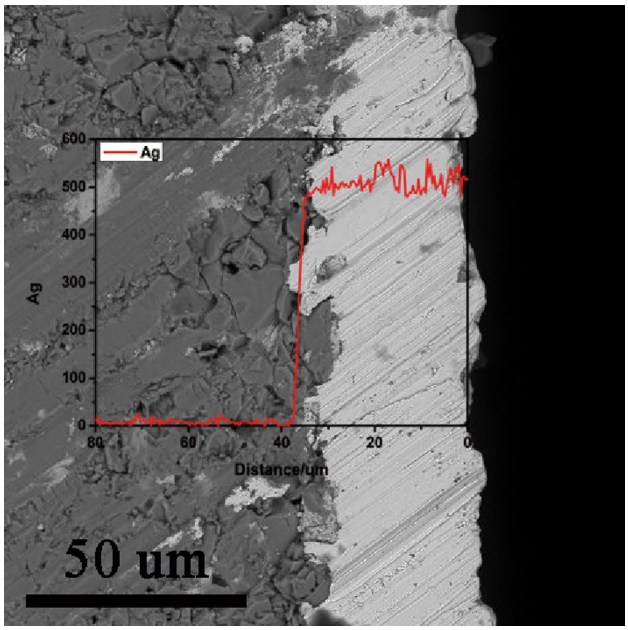

Fig. 7 SEM and EDS line scan of the cross-section of the L_2ZT_3–BLMT–TiO_2 (x = 2) composite co-fired with Ag electrode at 910 °C for 2 h

contents. However, the Q × f value of the composites not only is related to the phase composition and their relative contents but also is closely associated with microstructure such as the grains uniformity and grains size [8, 19, 20, 25], which result in the non-linear relationship between the Q × f value and relative contents.

In order to confirm the chemical compatibility of the composite with Ag electrode, the well-mixed powder of the L_2ZT_3–BLMT–TiO_2 (x = 2) composite mixes with 95% ethyl alcohol and xylene as solvent, Herring oil as dispersant, benzyl butyl phthalate (S160) as plasticizer and Poly(vinyl butyral) B-98 (PVB-B98) as binder to obtain slurry. After planetary-milling in aluminum jar for 2 h and vacuuming, the flat and astomatous green tape is prepared using tape-casting the slurry with a thick of 600 μm by doctor blade. The silver conducting plate (Shanghai Miracle Materials Technology Co. LTD.) is printed onto the LTCC green sheet by 200 mesh sieve. The printed LTCC green sheets (3 layers) are laminated, hot isostatic laminated and cut. Last, the components are sintered at 910 °C for 2 h in air at a heating rate of 5 °C/min, after burning out organics completely at 450 °C for 12 h. It is can be seen from cross-section of composite and Ag electrode film that there is a clear interface between the composite and the Ag electrode film, as shown in Fig. 7. And the EDS line scan shows that Ag diffusion no occur during the co-fired processing. The results mean that the composite has good compatibility with Ag electrodes. Combining the lower sintering temperature and excellent microwave dielectric properties, it can be proposed that the composites is a very promising candidate material for the LTCC applications.

4 Conclusions

In this study, the sintering behavior, activated energy, phases, microstructure and dielectric properties of the 5 BLMT–(95-x) $Li_2ZnTi_3O_{8-X}$ TiO_2 (x = 0, 1, 2, 3, 4 and 5, in wt%) composites LTCC materials had been investigated. The results indicate that all composites could be sintered at 910 °C for 2 h. The sintering activation energy of $Li_2ZnTi_3O_8$ ceramic is reduced from 520.9 ± 40.46 to 330.98 ± 47.34 kJ/mol by adding the BLMT glass additive. $Li_2ZnTi_3O_8$ and TiO_2 stably exist in sample and BLMT glass crystallizes forming $LaBO_3$ phase during sintering process. Corresponding to the increase of x in system, the temperature coefficient of resonant frequency of the composites was modified from − 12.94 to + 12.31 ppm/°C and τ_f of composite is zero the x value is 2.28, meanwhile the dielectric constant increases 24.5 to 26.5 and the Q × f value demonstrates gradually decrease 37,700–29,000 GHz. Optimized microwave dielectric properties of composites with x = 2 are obtained by sintering at 910 °C/2 h with: $\varepsilon_r = 25.3$, Q × f = 32,800 GHz, and $\tau_f = -0.54$ ppm/°C. Moreover, the composite is chemically compatible with Ag electrode at its sintering temperature, which makes it as a potential candidate for LTCC technology application.

References

1. Y. Imanaka, *Multilayered Low Temperature Cofired Ceramics (LTCC) Technology* (Springer, New York, 2005)
2. M.T. Sebastian, H. Wang, H. Jantunen. Curr. Opin. Solid. State Mater. **20**, 151–170 (2016)
3. M.T. Sebastian, R. Ubic, H. Jantunen, Int. Mater. Rev. **60**, 392–412 (2015)
4. S. George, M.T. Sebastian., J. Am. Ceram. Soc. **93**, 2164–2166 (2010)
5. P. Zhang, Y.G. Zhao, Ceram. Int. **42**, 2882–2886 (2016)
6. X.P. Lu, Y. Zheng, B. Zhou, Z.W. Dong, P. Cheng, Ceram. Int. **39**, 9829–9833 (2013)
7. X.P. Lu, Y. Zheng, Z.W. Dong, P. Cheng, R. Lin, Ceram. Int. **40**, 7087–7092 (2014)
8. Y.X. Li, H. Li, B. Tang, Z.J. Qin, H.T. Chen, S.R. Zhang, J. Mater. Sci.: Mater. Electron. **26**, 1181–1185 (2015)
9. C.H. Su, Y.D. Ho, C.L. Huang, J. Alloy. Compd. **607**, 67–72 (2014)
10. H.S. Ren, X.G. Yao, T.Y. Xie, M.Z. Dang, H.Y. Peng, S.H. Jiang, X.Y. Zhao, H.X. Lin, L. Luo, J. Mater. Sci.: Mater. Electron. **28**, 18646–18655 (2017)
11. H.S. Ren, S.H. Jiang, M.Z. Dang, T.Y. Xie, H. Tang, H.Y. Peng, H.X. Lin, L. Luo, J. Alloy. Compd. **740**, 1188–1196 (2018)
12. H.S. Ren, T.Y. Xie, M.Z. Dang, S.H. Jiang, H.X. Lin, L. Luo, Ceram. Int. **43**, 12863–12869 (2017)
13. V.B. John, *Introduction to Engineering Materials*, 3rd edn. (Macmillan, Houndmills, 1992)

14. V.K. Sing, J. Am. Ceram. Soc. **64**, 133–136 (1981)
15. Y.M. Lai, C.Y. Hong, L.C. Jin, X.L. Tang, H.W. Zhang, X. Huang, J. Li, H. Su, Ceram. Int. **43**, 16167–16173 (2017)
16. C.L. Huang, W.R. Yang, P.C. Yu, J. Eur. Ceram. Soc. **34**, 277–284 (2014)
17. L. Hao, G.J. Shu, F.C. Meng, H.X. Lin, Ceram. Int. https://doi.org/10.1016/j.ceramint.2018.04.136
18. X.Y. Chen, S.X. Bai, M. Li, W.J. Zhang., J. Eur. Ceram. Soc. **33**, 3001–3006 (2013)
19. Y.X. Li, J.S. Li, B. Tang, S.R. Zhang, H. Li, Z.J. Qin, H.T. Chen, H. Yang, H. Tu, J. Mater. Sci.: Mater. Electron. **25**, 2780–2785 (2014)
20. G.H. Chen, M.Z. Hou, Y. Bao, C.L. Yuan, C.R. Zhou, H.R. Xu, Int. J. Appl. Ceram. Technol. **10**, 492–501 (2013)
21. M. He, H.W. Zhang, J. Mater. Sci.: Mater. Electron. **24**, 3303–3308 (2013)
22. Y.X. Li, Z.J. Qin, B. Tang, S.R. Zhang, G. Chang, H. Li, H.T. Chen, H. Yang, J.S. Li, J. Electron. Mater. **44**, 281–286 (2015)
23. M.Z. Hou, G.H. Chen, Y. Bao, Y. Yang, C.L. Yuan, J. Mater. Sci.: Mater. Electron. **23**, 1722–1727 (2012)
24. X.P. Lu, Y. Zheng, Z.W. Dong, Q. Huang, Mater. Lett. **131**, 1–4 (2014)
25. K. Zhang, L. Yuan, Y.P. Fu, C. Yuan, W. Li., J. Mater. Sci.: Mater. Electron. **26**, 6526–6531 (2015)